Applied Surface Science 363 (2016) 286–295

Contents lists available at ScienceDirect

Applied Surface Science

journal homepage: www.elsevier.com/locate/apsusc

Osseointegration properties of titanium dental implants modified with a nanostructured coating based on ordered porous silica and bioactive glass nanoparticles

Cristian Covarrubias[a,*], Matías Mattmann[a], Alfredo Von Marttens[b], Pablo Caviedes[c], Cristián Arriagada[c], Francisco Valenzuela[a], Juan Pablo Rodríguez[d], Camila Corral[e]

[a] Laboratory of Nanobiomaterials, Institute for Research in Dental Sciences, Faculty of Dentistry, University of Chile, Santiago, Chile
[b] Department of Prosthesis, Faculty of Dentistry, University of Chile, Santiago, Chile
[c] Laboratory of Cell Therapy, ICBM, Faculty of Medicine, University of Chile, Chile
[d] Laboratory of Cell Biology, INTA, University of Chile, Santiago, Chile
[e] Department of Restorative Dentistry, Faculty of Dentistry, University of Chile, Santiago, Chile

ARTICLE INFO

Article history:
Received 6 July 2015
Received in revised form
22 September 2015
Accepted 1 December 2015
Available online 8 December 2015

Keywords:
Titanium implant
Osseointegration
Nanotopography
Nanobioactive glass
Bone

ABSTRACT

The fabrication of a nanoporous silica coating loaded with bioactive glass nanoparticles (nBG/NSC) on titanium dental implant surface and its *in vitro* and *in vivo* evaluation is presented. The coating was produced by a combined sol–gel and evaporation induced self-assembly process. *In vitro* bioactivity was assessed in simulated body fluid (SBF) and investigating the osteogenic differentiation of human bone marrow mesenchymal stem cells (hBMSCs). A rat tibial model was employed to analyze the bone response to nBG/NSC-modified titanium implant surface *in vivo*.

The nBG/NSC coating was confirmed at nano level to be constituted by a highly ordered nanoporous silica structure. The coating nanotopography in conjunction with the bioactivity of the BG particles accelerate the *in vitro* apatite formation and promote the osteogenic differentiation of hBMSCs in absence of osteogenic supplements. These properties accelerate the formation of bone tissue in the periphery of the implant after 3 weeks of implantation. Backscattered scanning electron microscopy images revealed the presence of gaps and soft tissue in the unmodified implant after 6 weeks, whereas the nBG/NSC-modified implant showed mature bone in intimate contact with the implant surface. The nBG/NSC coating appears promising for accelerating the osseointegration of dental implants.

1. Introduction

Dental implants have become a widely accepted and predictable treatment to replace single or multiple missing teeth [1,2]. Although they present an elevated clinical success rate [3], efforts are made in order to obtain faster and more stable osseointegration, which has stimulated greatly the developments on implant design [4,5]. Different strategies have been established including the treatment of the surface of the implant to create physical and chemical changes [6].

Nowadays, most of the commercially available dental implants have surface modifications in order to increase their surface roughness [7]. Several studies have observed a positive effect on modifying the surface topography of implants compared to smooth surfaces [8]. However, majority of current commercially available implant present surface morphologies that are controlled only to the micron level, though the events involved in osseointegration occur in a nanoscale setting [7,9]. Therefore, it is possible that understanding and controlling tissue responses at the nano level, by providing nanoscale topography to dental implants, could help to eliminate rejection and improve osseointegration processes [9,10].

Different techniques have been developed to produce surface modifications at the nano level on implants [10], including optical lithography [11], crystal deposition [12], and chemical treatment [13], among others. However, the use of these methods makes difficult to control the distribution and homogeneity of nanostructures on the implant surface. The use of novel techniques derived from soft matter physical chemistry and inorganic or hybrid sol–gel chemistry allows a high control of material nanostructure. By using the evaporation-induced self-assembly (EISA) technique, in which colloids self-organize into ordered layers during evaporation of the solvent [14], together with sol–gel processing is feasible to achieve

* Corresponding author at: Sergio Livingstone 943, Independencia, Santiago, Chile.
E-mail address: ccovarrubias@odontologia.uchile.cl (C. Covarrubias).

http://dx.doi.org/10.1016/j.apsusc.2015.12.022
0169-4332/

regularly-patterned nanoporous surfaces [15,16]. This method is simple, inexpensive, scalable, and has a high reproducibility. In a previous study, we demonstrated that titanium surfaces modified with silica coatings with highly ordered sub-10 nm porosity produced by EISA/sol–gel technique improves the osteoblast adhesive responses and stimulates the osteogenic differentiation of stem cells, probably through a mechanotransduction mechanism [17]. On the other hand, the loading of the implant surface with bioceramic particles also constitutes a common approach to accelerate the osseointegration process. The most commonly tested are calcium phosphate (hydroxyapatite and tricalcium phosphate) and bioactive glasses, which when in contact with fluids tend to form a carbonated apatite layer, similar to the mineral phase of osseous tissue [9]. Several studies have reported a higher rate and extent of bone formation adjacent to implants coated with microsized bioceramics than in uncoated implants [18,19]. Bioceramic nanoparticles are expected to have improved bioactive properties, due to the higher aspect ratio exhibited by the nanodimensional materials. In a previous study, we compared the ability of hydroxyapatite and bioactive glass nanoparticles to induce the formation of apatite, finding that bioactive glass nanoparticles produce a faster formation of apatite in physiological medium [20]. It is expected that the incorporation of bioactive glass nanoparticles into the patterned nanoporous silica coating could generate a novel nanocomposite coating material combining the osteogenic properties of the porous nanotopography with the chemical bioactivity of the ceramic nanoparticles.

The aim of this work is to prepare a highly ordered nanoporous silica coating loaded with bioactive glass nanoparticles (nBG/NSC) on titanium implant surfaces and assess the osseointegration properties of the modified surface. It is hypothesized that this nanostructured coating stimulate the bone-like apatite mineralization and the osteogenic differentiation of stem cells, thus accelerating the formation of bone in intimal contact with the implant surface. The *in vitro* bioactive response of the modified titanium surfaces was evaluated on apatite formation in simulated body fluid (SBF) and on osteogenic differentiation of stem cells. In addition, the *in vivo* osseointegration process of titanium implants modified with the novel nanostructured coating was assessed by using rat tibial model.

2. Material and methods

2.1. Synthesis of nBG/NSC-modified titanium surfaces

Nanoparticles of bioactive glass (nBG) were synthesized by the sol–gel method using the following molar composition: $58SiO_2$:$40CaO$:$5P_2O_5$ reported in a previous work [20]. nBG/NSC modified titanium surfaces were prepared on sheets of Ti_6A1_4V titanium alloy (Zimmer Dental) using the EISA sol–gel technique. Titanium sheets ($15 \times 15 \times 1$ mm) were sanded with silicon carbide paper (800 grit) and cleaned ultrasonically with acetone and ethanol before use. The coating sol solutions were prepared using the amphiphilic triblock copolymer Pluronic P123 (P123; $EO_{20}PO_{70}EO_{20}$, Mw 1/4 5800; Aldrich) as pore structure-directing agent (SDAs). Briefly, 3.7 g of tetraethyl orthosilicate (98%; Aldrich) were prehydrolyzed in a solution containing 10 mL of ethanol (95%) acidified with 0.5 mL of HCl 0.5 N (pH 2.0) under vigorous stirring at room temperature for 20 min. Appropriate amount of nBG were added into 10 mL ethanol to produce a 10 wt.% suspension. Both solutions were added to a solution containing 2 g of P123 dissolved in 20 mL of ethanol. The resulting solution was then submitted to an aging period at room temperature for 24 h with stirring, and films were prepared by slip coating on the titanium sheets.

For the slip-coating procedure the titanium sheet was suspended in an inverted position with a pair of tweezers attached to a clamp fixed loosely enough to a stand to allow rotation of the tweezers. The polished side was brought in contact with the silica sol. The titanium sheet was kept in this half-immersed position for 20 s, slipped away horizontally by rotating the tweezers, and then dried in a vertical position for 40 s. The silica coatings were kept for 24 h at 35 °C, and then calcined by heating at a rate of 0.5 °C/min to 400 °C, holding that temperature for 4 h to remove the SDA.

In the case of *in vivo* animal study, orthodontic titanium mini-implants (Biomaterials Korea®, Ti_6A1_4V) with 1.5 mm in diameter and 7 mm in length were used. The implants were coated using a dip-coating procedure. For this purpose, the implants were suspended in an inverted position with a device that allows vertical movement. The implants were kept in the sol during 1 min and then vertically removed at a 0.3 mm/s speed using a precision micro-geared motor. The coated implants were kept for 24 h at 35 °C, and then calcined, by heating at a rate of 0.5 °C/min and holding it for 4 h at 400 °C. After that, implants were sterilized for 1 h with UV light and then kept in sterile containers.

2.2. Materials characterization

The unmodified and nBG/NSC-modified titanium sheet and implant surfaces were examined by scanning electron microscopy (SEM; Zeiss, DMS 940) after coating the surfaces with gold. The structural order of the porous silica coatings was analyzed by low-angle X-ray diffraction (XRD) within a 2θ range of 0.5–5°. XRD patterns were collected on a Siemens D 5000 diffractometer using Cu Kα radiation at a scanning speed of 0.2°/min. The porous nanostructure was examined by high-resolution transmission electron microscopy (HR-TEM) on a FEI-Tecnai G2 F20 S-Twin high-resolution transmission electron microscope equipped with a field emission gun operating at an accelerating voltage of 120 kV. The specific apparent surface areas (Sg) of coating material was measured by N_2 adsorption at 77 K in a Micromeritics ASAP 2010 sorptometer and calculated using the Brunauer–Emmett–Teller (BET) equation.

2.3. In vitro *bioactivity assays*

The ability of the nBG/NSC modified titanium surfaces to induce the formation of apatite was assessed in acellular SBF, which has inorganic ion concentrations similar to those of human extracellular fluid. The SBF solution was prepared according to the procedure described elsewhere [21] using the standard ion composition (Na^+ 142.0, K^+ 5.0, Mg^{2+} 1.5, Ca^{2+} 2.5, Cl^- 147.8, HCO_3^- 4.2, HPO_4^{2-} 1.0, SO_4^{2-} 0.5 mM). The fluid was buffered at physiological pH 7.4 at 37 °C with tri-(hydroxymethyl) aminomethane and hydrochloric acid. The unmodified and nBG/NSC modified titanium sheets (1.5 cm^2) were individually soaked in 20 mL of SBF in polyethylene containers at 36.5 °C using a thermostatic bath. After incubation for 3 days, the samples were removed from the SBF, rinsed with distilled water, and dried at 60 °C. Apatite mineralization on the surfaces was analyzed by SEM with a Jeol JSM 5410 microscope equipped with energy-dispersive X-ray spectroscopy (EDX). The structural order of the surfaces was analyzed by low-angle XRD, collected on a Siemens D 5000 diffractometer using Cu Kα radiation at a scanning speed of 0.2°/min.

2.4. Cell culture

Human bone marrow stem cells (hBMSCs) were used to evaluate the osteogenic differentiation capacity of the nBG/NSC-modified titanium surfaces. Approximately $1 \times 10^3/cm^2$ cells were seeded on sterilized unmodified and nBG/NSC-modified titanium sheets (10 mm × 10 mm) and maintained at 37 °C in a humidified air atmosphere containing 5% CO_2, in Dulbecco's modified Eagle medium

(DMEM; Invitrogen Life Technologies). The medium was supplemented with 10% PBS, 100 IU/mL penicillin and 100 μg/mL streptomycin and it was changed every 3–4 days. After 15 days of culture, mineralized nodule formation on the titanium surfaces was examined by SEM and nodule composition analyzed by EDX. For this purpose, adherent cells were fixed in 2.5% glutaraldehyde, then progressively dehydrated in ethanol, dried in supercritical CO_2, and coated with gold for SEM observation (Zeiss, DMS 940).

2.5. In vivo *experiment*

2.5.1. *Surgical implantation*

In vivo experiments were conducted in a total of 11 Sprague-Dawley adult rats, according to the codes and rules of the Ethics Committee of the Faculty of Medicine of University of Chile, taking care of surgical procedures, pain control, standards of living and appropriated death.

Implant surface effects on early osseointegration was evaluated using a rat tibia model [22,23]. Rats were anaesthetized with ketamine and xylazine previous to the surgical procedure. The region of the surgery was shaved and disinfected. Implants were placed unilaterally in the proximal tibial metaphysis of the rats with a flapless technique [24,25], consisting of drilling through skin to bone using a hand drill with a 1.2 mm diameter bur. During perforation the site was profusely irrigated with physiological saline solution for cleaning and refrigeration purposes. The implant was introduced in the perforation through manual torque and the wound was covered with a patch, to avoid the animal biting or scratching it. Post-surgical position of the implant was verified by conventional X-ray radiography. After 3 and 6 weeks the animals were sacrificed with an overdose of intraperitoneal ketamine and xylazine.

2.5.2. *Sample processing*

Samples of tissue/implant region were obtained after 3 and 6 weeks of implantation. The samples were fixed in 10 wt.% formaldehyde for 48 h, and then immersed in ascending concentrations of alcohol. Samples were then embedded in methyl methacrylate (PMMA) without decalcification [26], using progressively increasing PMMA solutions (solutions of acetone:PMMA with 1:2, 1:5, 1:10 ratio, immersing the sample for 1 h in each solution), to finally obtain a 1 cm diameter PMMA block. The PMMA embedded blocks were cut with a low speed diamond blade saw (Isomet 1000, Buehler) in order to obtain 500 μm discs in thickness with a transversal cut of the tissue/implant interface.

2.5.3. *Histological analysis*

To observe and differentiate soft tissue, osteoid tissue, and mature bone, discs were stained with toluidine blue stain solution and observed with optical light microscopy (Axioskop, Zeiss). The area of newly formed bone within a circle of 200 μm width around the implant was calculated by using the analysis tools of Adobe Photoshop CS3.

The tissue/implant interface after 3 weeks of implantation was observed with back-scattered electrons scanning electron microscopy (BSE-SEM, Jeol 6360 LV), which allows differentiating regions with different mineralization degrees. Elemental analysis was performed with an EDX microanalysis (EDX, Jeol 6360 LV).

3. Results

3.1. *Preparation of nBG/NSC-modified titanium surfaces*

SEM images taken on the unmodified and nBG/NSC-modified titanium surfaces were obtained (Fig. 1a and b). The coating layer appears uniform, smooth and without micro defects, whereas nBG nanoparticles can be observed as micro-sized aggregates into the silica matrix. The nanostructural order of nBG/NSC-modified titanium was analyzed by XRD (Fig. 1c). The XRD pattern of nBG/NSC-modified titanium surfaces presents the characteristic reflections around 2.3° corresponding to a highly ordered hexagonal mesoporous structure. The low-angle XRD reflections are the result of an ordered hexagonal array of the cylindrical pores, which is indexed assuming a hexagonal unit cell (space group *p6mm*) [27]. HR-TEM image (Fig. 1d) shows the highly organized surface topography, consisting of hexagonal porous of *ca.* 6.5 nm diameter, oriented perpendicular to the titanium surface. This nanostructured porous coating material presented a BET specific surface area of 419 m^2/g.

3.2. In vitro *bioactivity assay*

For a preliminary evaluation of the bioactivity of the nBG/NSC modified titanium sheet, *in vitro* testing was performed in SBF. SEM images reveal scarce mineral deposits on unmodified titanium (Fig. 2a) after 3 days of immersion in SBF, however nBG/NSC modified titanium (Fig. 2b) exhibit a higher degree of mineralization on its surface. EDX elemental analysis of the nBG/NSC modified titanium sheets (Fig. 2d) shows the presence of Ca and P, which was not detected on the unmodified titanium surface (Fig. 2c). XRD pattern of the nBG/NSC modified titanium surface (Fig. 2e) presents reflections at 27° and 31.7°, which are attributed to the apatitic nature of the mineral deposits.

3.3. *hBMSC differentiation*

Fig. 3 shows the SEM image of hBMSC cultured on unmodified and nBG/NSC modified titanium surface for 15 days. Cells cultured on both surfaces revealed a consistent growth, covering most of the titanium surface, with flattened and extended cellular processes that attach to both substrates (Fig. 3a and c). However, cells grown on unmodified titanium surface did not show the presence of mineralized nodules, as it was observed on the SEM image of hBMSC grown on nBG/NSC modified titanium surface. EDX elemental analysis (Fig. 3e) of the mineral nodule detected on the nBG/NSC modified titanium surface, shows an elevated Ca and P content.

3.4. In vivo *animal study*

Commercial titanium implants were modified with nBG/NSC coating by using an optimized dip-coating procedure. SEM images of the nBG/NSC-modified titanium implant surface are shown in Fig. 4. The nBG/NSC modified implant shows a continuous and homogeneous surface, without exposure of the titanium surface (Fig. 4a and b). Nanoparticles incorporated into the coating can be also observed as micrometric agglomerations of approximately 0.5–2.5 μm in size (Fig. 4c).

The radiography in Fig. 4d shows the location of the implants placed on the proximal tibial metaphysis of the rat.

3.5. *Histological analysis*

Fig. 5 shows the histological images taken on the metal/tissue interface. It is possible to observe the implant (circumferential black area), mature bone (in blue color), and the new bone tissue/osteoid (in light pink and purple color) around the implants.

After 3-week implantation (Fig. 5a–d), the samples showed marked differences in the tissue/implant interface between the unmodified (Fig. 5a and b) and the modified titanium implants (Fig. 5c and d). nBG/NSC-modified titanium implant reveals greater amount of mature bone (in blue color) surrounding it, in comparison to the unmodified implant, with a majority of soft/fibrous

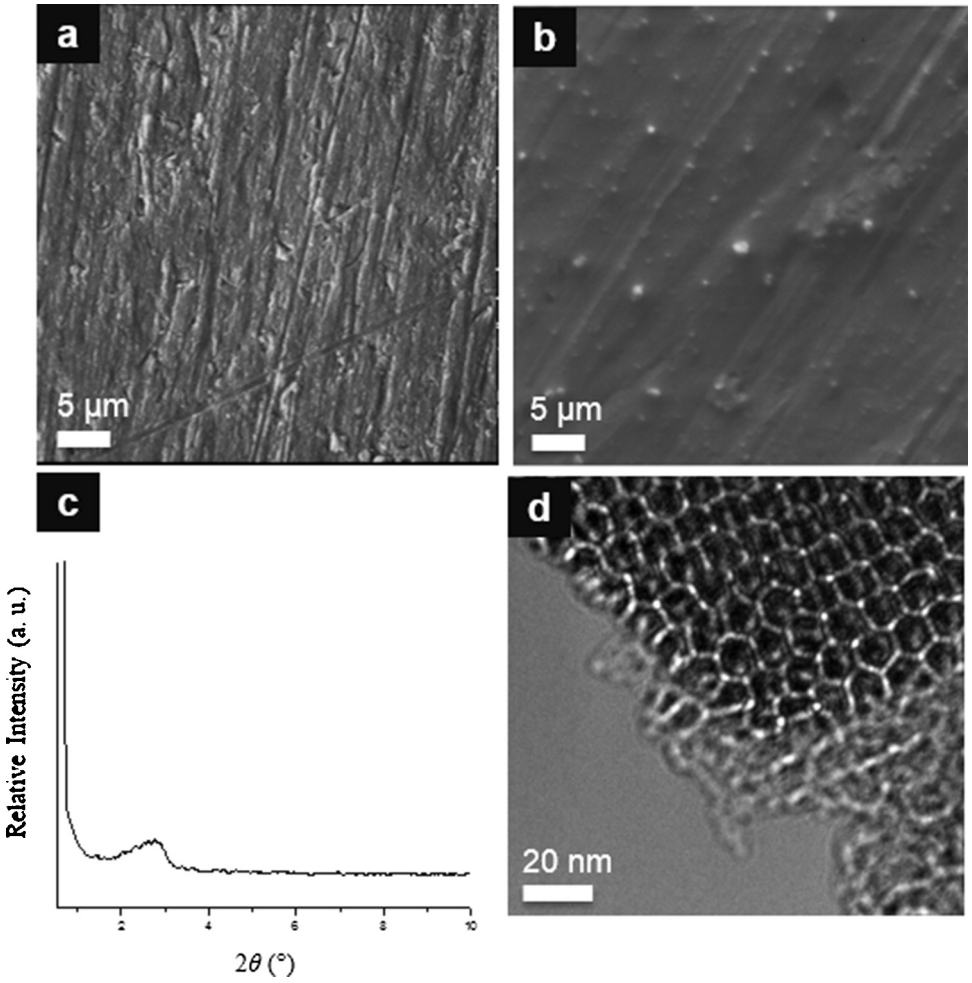

Fig. 1. SEM images of: (a) unmodified titanium surface, and (b) nBG/NSC-modified titanium surface. (c) XRD pattern of nBG/NSC-modified titanium surface. HR-TEM image of: (d) the highly ordered nanoporous structure of nBG/NSC coating.

tissue around the implant and less amount of mature bone. Samples obtained after 6 weeks of implantation (Fig. 5e–h) in comparison to the 3-weeks images, showed a more complete presence of mature bone surrounding the implants, both for the unmodified as for the nBG/NSC-modified titanium implant. However, in the case of the unmodified titanium implant sample, it is observed a considerable amount of gaps (*ca.* >50 μm), with presence of soft/fibrous tissue, and osteoid tissue. Conversely, the nBG/NSC-modified titanium implant sample showed a complete presence of mature bone covering the whole implant surface. Area measurements of newly formed bone around of the implants (Table 1), confirm the significantly larger bone growth in the periphery of the nanoscale-modified implant.

Due to that the unmodified and modified titanium implant/tissue interface after 3 weeks of implantation exhibited greater differences in the degree of bone maturation when observed with histological staining, this time point was chosen to analyze by BSE-SEM and EDX the tissue in intimate contact with the implant. Fig. 6 shows BSE–SEM images; more mineralized areas are shown in a brighter shade, while soft tissues are seen in darker color. The nBG/NSC-modified titanium implant/tissue interface (Fig. 6a) showed greater presence of highly mineralized tissue closely bounded to the implant surface compared to unmodified titanium implant (Fig. 6b). EDX elemental analysis of selected areas (Fig. 6b and d), show the main elements found in the tissue grown closely to the implant surface. The predominant elements were Ca and P, which correspond to the main elements of the mineralized bone tissue. The contents of Ca and P were significantly higher in the tissue grown on nBG/NSC-modified implant, compared to the unmodified implant. The highest carbon content was found in the tissue grown on the unmodified implant.

Table 1
Area values of newly formed bone around unmodified and nBG/NSC-modified implant after 3 and 6 weeks of implantation.

	Bone area (μm²)	
	3 weeks	6 weeks
Unmodified implant	62,108	677,726
nBG/NSC-modified implant	740,365	1,134,247

4. Discussion

This study demonstrates the synthesis of a novel nanocomposite coating for titanium surfaces, which combines the osteogenic properties of a porous nanotopography with the chemical bioactivity of nBG. In addition, it shows a faster mature bone deposition around nBG/NSC-modified titanium implants *in vivo*, on a rat model, compared to unmodified titanium implants.

The synthesis of the composite coating based on nanoporous silica loaded with nBG on titanium surfaces were achieved using the combined EISA/sol–gel technique. The silica coating loaded with nBG particles showed to be uniform and without micro defects, and at the nano level the formation of the highly ordered nanoporous

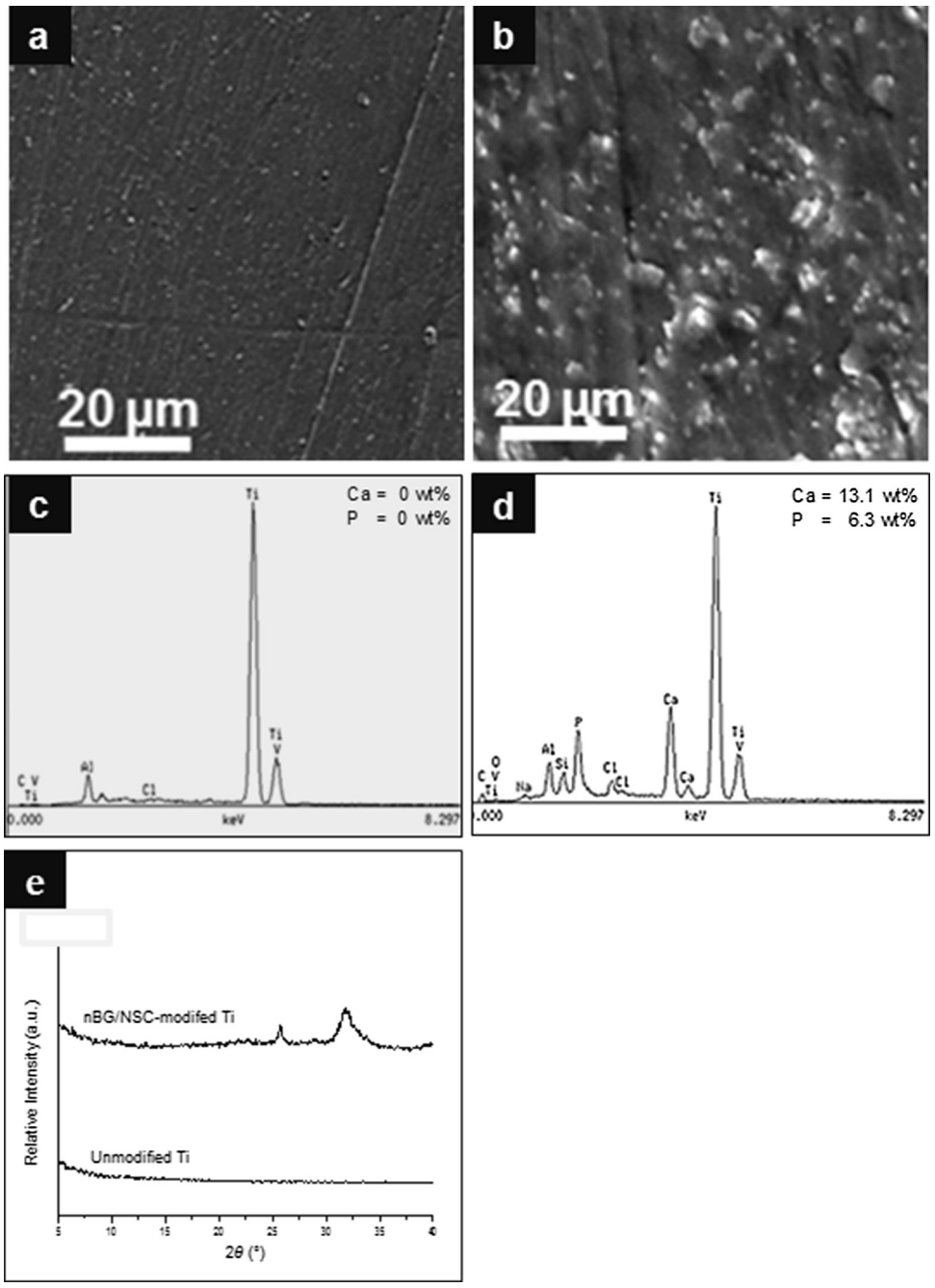

Fig. 2. SEM images of titanium surfaces after 3 days of immersion in SBF: (a) unmodified titanium, (b) nBG/NSC-modified titanium, with its corresponding EDX elemental analysis pattern (c) unmodified titanium, (d) nBG/NSC-modified titanium and (e) XRD pattern of both surfaces.

silica structure was confirmed. These results demonstrate that the incorporation of nBG into the silica coating does not cause an alteration of the ordered nanoporous structure, which on a previous study proved to stimulate the cell adhesion and differentiation processes [17]. EISA sol–gel technique offers finer control of the nanostructure [15], as compared to previously reported methods used for modifying the topography of titanium surfaces such as plasma spraying, grit-blasting or acid-etching, which in general do not enable the formation of uniform nanostructures [28]. In addition, EISA sol–gel has the added benefits of being a low-cost, simple and scalable technique, providing a high uniformity of the pattern created. Sol–gel coating also enables the attachment of nanoparticles on the titanium surface with a relatively homogeneous distribution.

Preliminary *in vitro* assessment of bioactivity in SBF revealed a higher degree of apatite mineralization on the nBG/NSC-modified titanium surface, in contrast to the absence of apatitic deposits on the unmodified titanium. This can be attributed to a combination of the effects of the physical nanotopography and chemical modifications due to the incorporation of nBG into the titanium coating. The high surface area provided by the nBG/NSC coating increases significantly the available surface for interaction with the simulated physiological media in comparison to unmodified titanium. A high-surface free energy is a known to be a factor that favors the process of apatite nucleation and growth in SBF [29,30]. On the other hand, the presence of nBG into the coating also increases the bioactive properties of the modified titanium surface. Bioactive glass is a material well-known by its ability to induce formation of

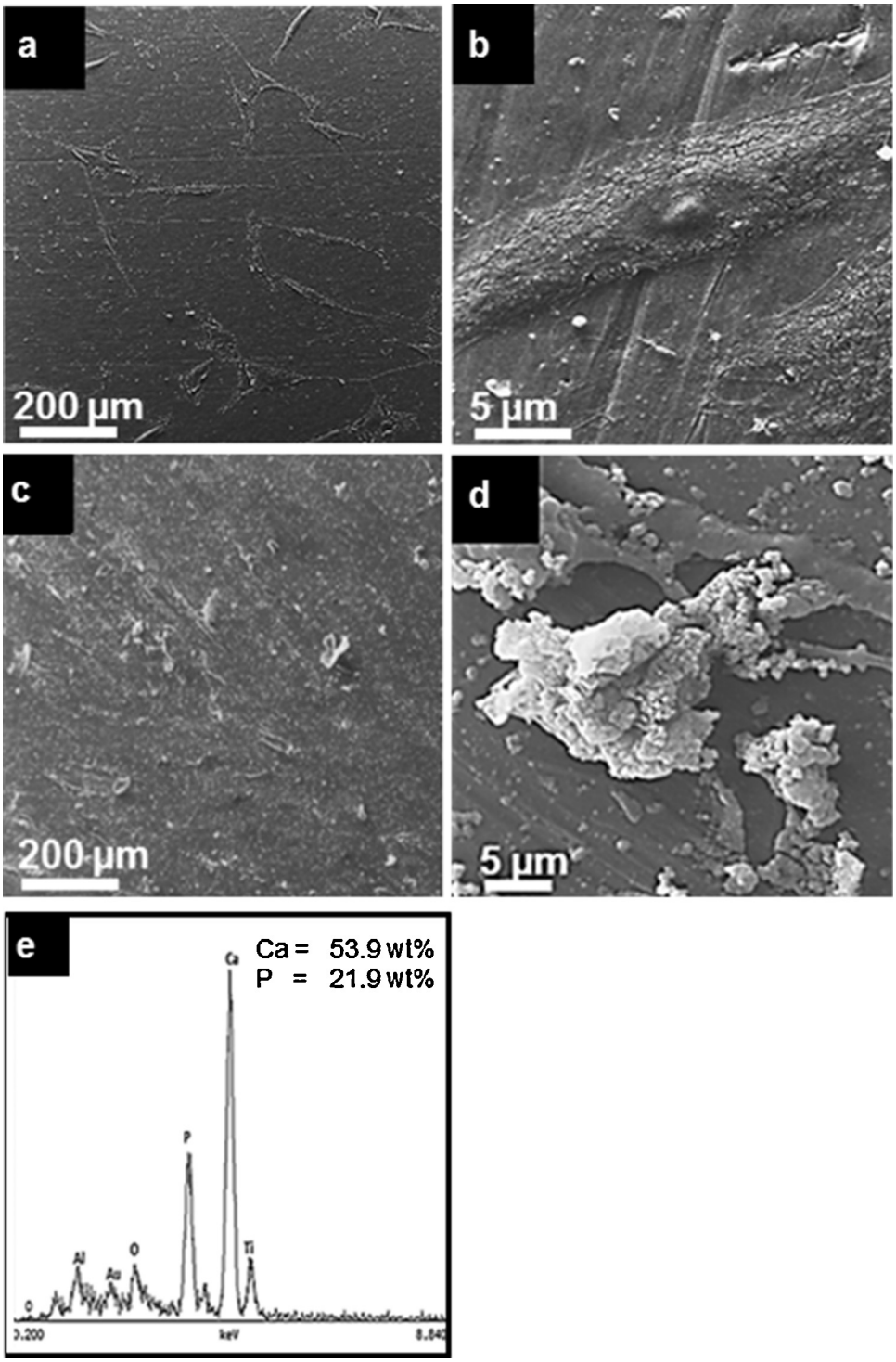

Fig. 3. SEM images of hBMSC after 15 days of culture on titanium surfaces: (a) unmodified titanium, (c) nBG/NSC-modified titanium. High magnification showing hBMSCs (b) cultured on the unmodified titanium and (d) associated with mineralized bone nodules on the nBG/NSC-modified titanium surface. (e) EDX analysis of mineralized nodule showed in (d).

bone-like apatite, particularly BG particles with nanometric dimensions having higher dissolution rate have demonstrated notably to accelerate this process when incorporated into different matrices [20,31–33].

The ability of the modified titanium surface to induce osteogenic differentiation of stem cells was assessed by analyzing the formation of bone nodules associated to hBMSC cultures. The nBG/NSC-modified titanium was able to stimulate the osteogenic differentiation of hBMSCs with abundant production of mineralized bone nodules in absence of osteogenic factors. The EDX chemical elemental analysis confirmed that the nodules have a high Ca and P content, which may correspond to partially crystallized apatite deposits or mineralized matrix vesicles produced during the cell-mediated bone formation process. Osteogenic differentiation of stem cells may be influenced by both the physical and chemical properties of the nBG/NSC-modified titanium surface. The nanostructure of implant surface can influence cell-implant interaction and tissue formation [34,35]. Several studies have shown,

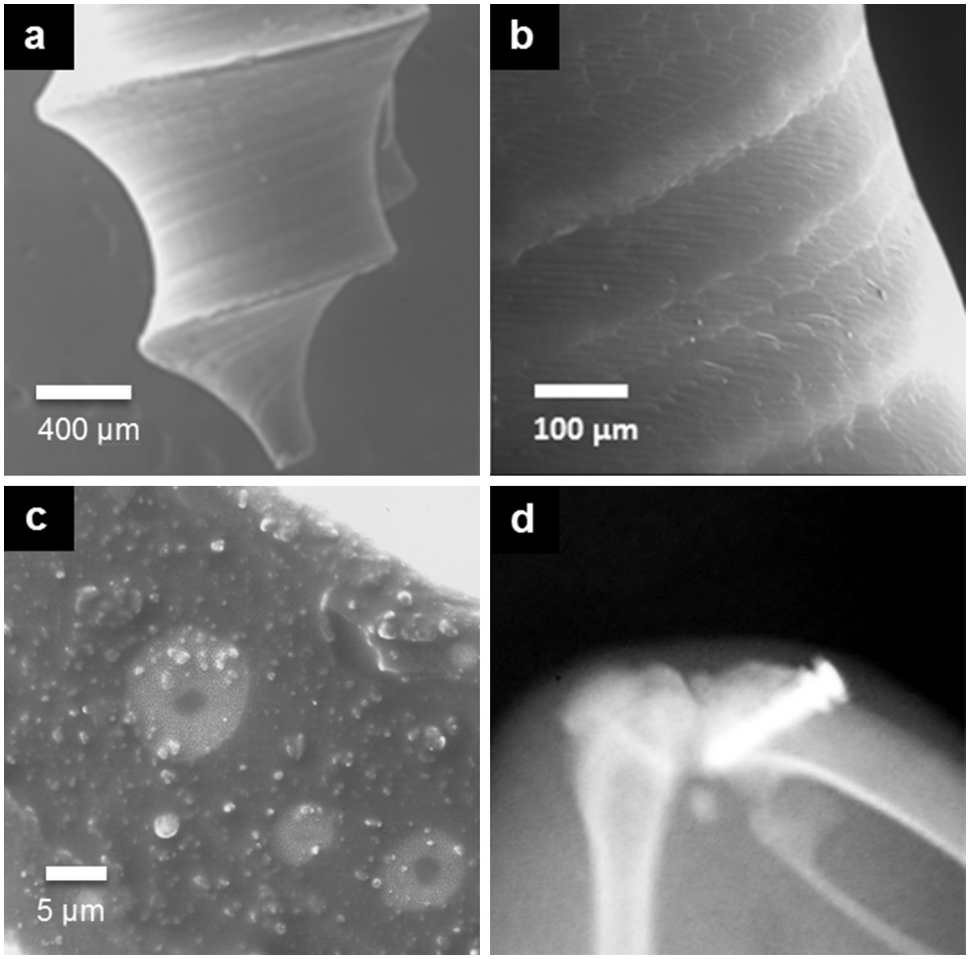

Fig. 4. SEM images of the nBG/NSC-modified titanium implant surface at (a) 50×, (b) 500× and (c) 2000×. (d) Anatomical position of the implant in the proximal tibial metaphysis of the rat, visualized by radiography.

in vitro, the differentiation of human bone marrow cells into the osteoblastic phenotype when exposed to nanoporous surfaces, in absence of osteogenic supplements [36–38]. In a previous work, we demonstrated that the silica coating with highly ordered sub-10 nm porosity is able to induce the osteogenic differentiation of stem cells [17]. Growing evidence suggests that mechanical signals from nanostructured surfaces are sensed by the cells through filopodial interaction, transmitted to the nucleus through the cytoskeleton, to modulate the expression of bone–specific transcription factors [35–38]. In addition, the chemical changes related to the incorporation of nBG can also influence osteogenic differentiation of stem cells. Through nBG ionic dissolution products, hBMSCc can chemically drive along the osteoblastic pathway, resulting in increased mineralizing activity [39,40]. Tsigkou et al. [41] have demonstrated that specific concentrations of ionic dissolution products of 45S5 Bioglass® recreate an extracellular environment that is capable of supporting osteoblast phenotype expression and extracellular matrix deposition and bone nodule mineralization in osteoblasts. In the current work, the BG particles with nanometric dimensions incorporated into the silica coating, could further accelerate the osteogenic differentiation process as recently demonstrated by our group [42] assessing BG particles with different nanodimensions.

The nanostructured nBG/NSC coating was also produced on the surface of commercial mini-implants. The EISA/sol–gel coating technique was optimized for the geometry and dimensions of the dental implants. The procedure showed to be effective in the formation of a continuous and homogeneous coating, with scarce presence of agglomerations of nBG. These coating characteristics contrast with those exhibited by other types of ceramic coatings fabricated on titanium implants, which normally produce uneven coating distributions, irregular surface morphology or disordered particle arrangements [18,43].

The osseointegration response of nBG/NSC-modified implants was assessed in a rat tibial model. This animal model has been proposed and utilized in previous osseointegration studies, since it provides evidence of rapid formation of bone adjacent to implant and shows comparable success rates to dental implants placed in humans [44]. Osseointegration, defined as direct contact, demonstrated at the resolution of light microscope, between living bone and the surface of a load-bearing implant, has been observed on this model after 6 weeks [45–47]. In the present study, the *in vivo* assessment of the modified titanium implants showed that, the nanostructured nBG/NSC coating, significantly improves the osseointegration properties of the implants. Within short time of implantation, after 3 weeks, it was observed that the modified-titanium implant accelerates the formation of mature bone tissue around the implant, compared to unmodified implants. This response should be the consequence of the capability of this surface modification to induce the deposit of apatite-like minerals on its surface; and to promote the osteogenic cell differentiation, as it was observed previously on the *in vitro* part of this work. Particularly, the nanotopography of the modified implant can mimic the extracellular matrix, whose components are generally of nanometer size [9]. This characteristic enhances adhesion of proteins, facilitating the migration of osteogenic cells to its surface and thus the rate of osseointegration, favoring a direct bone-implant

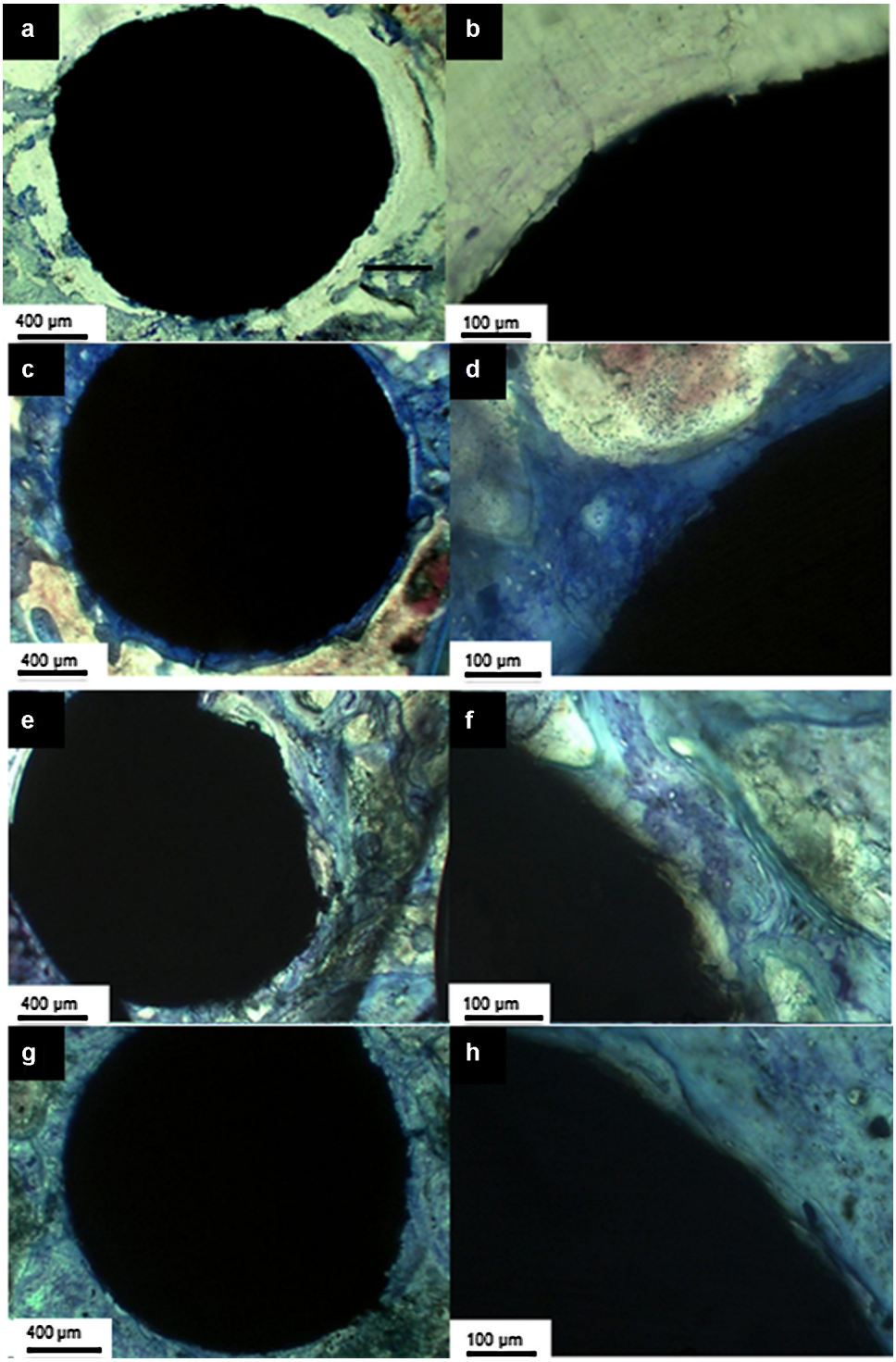

Fig. 5. Histological images of tissue/implant interface stained with toluidine blue after 3 weeks (a–d) and 6 weeks of implantation (e–h). The unmodified (a, b, e and f) and nBG/NSC-modified (c, d, g and h) titanium implants/tissue interface images are shown with different magnification. (For interpretation of the references to color in the text, the reader is referred to the web version of the article.)

contact without the presence of an interfering connective tissue layer [9,28]. Higher resolution images by using BSE–SEM after 6 weeks revealed the presence of gaps and soft tissue in the unmodified implant, whereas the modified implant showed complete mature bone presence in intimate contact with the implant surface. This accelerated osseointegration process was also evidenced by a higher degree of bone mineralization (greater contents of Ca and P), and a lower C content on the tissue adjacent to the implant, which could be associated with the lower presence of organic fibrous tissue in the interface observed with histological staining, when compared to the unmodified implant. Wheeler et al. [18] found that the bone ingrowth for an implant coated with 45S5 Bioglass® did not exhibited significant differences with respect to the control after 4 weeks of healing. Ballare et al. [48] reported the preparation of nonporous silica coating containing 10 wt.% of commercial wollastonite particles on surgical stainless steel implants. This sol–gel coating promoted the formation and growth of a new bone in the periphery of the implant after 60 days, although the newly

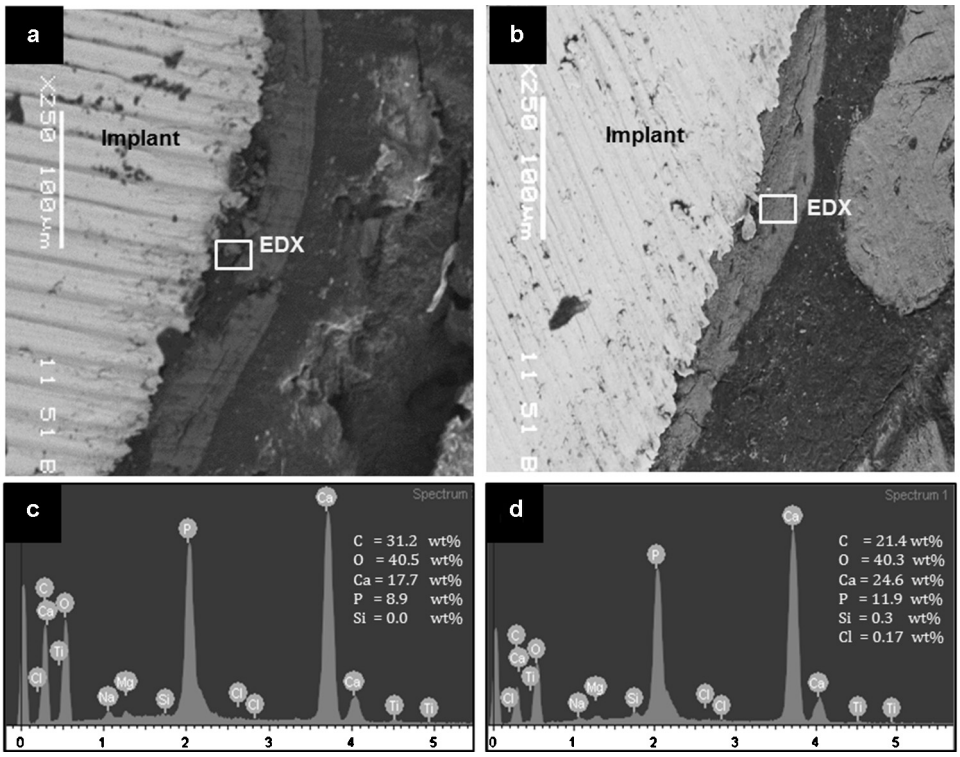

Fig. 6. BSE–SEM images of tissue/implant interfaces: (a) tissue/unmodified implant and (b) tissue/nBG/NSC-modified implant after 3 weeks of implantation. EDX elemental analysis of selected interface regions between the newly formed bone and the (c) unmodified and (d) nBG/NSC-modified implants.

formed bone was not completely mature, presenting osteocytes and some osteocyte lacunae. In our study, the mechanical stimulus from the highly ordered nanoporous topography of the silica coating in combination with the improved bioactivity of the nanosized BG particles should be responsible of the faster osseointegration response observed. The results of this work demonstrate the effect of the control of the implant nanoscale structure in modulating the biological response, with possible clinical consequences in the performance of the implant-supported rehabilitation treatments.

5. Conclusions

This study demonstrates the feasibility of modifying titanium surfaces with a highly ordered nanoporous silica coating loaded with bioactive glass nanoparticles. It also shows the possibility to achieve the same surface modification, with an optimized technique, on commercial titanium implants. The coating nanotopography in conjunction with the chemical bioactivity of the nanoparticles enhance the *in vitro* bone-like apatite formation and stimulate the osteogenic differentiation of stem cells in absence of osteogenic supplements. These properties allow improving the osseointegration responses *in vivo*, accelerating the formation of bone tissue in intimate contact with the implant surface within a short time of implantation.

The nanostructural modification developed in this work appears as a promising alternative to improve the osseointegration properties of titanium dental implants.

Acknowledgments

The authors acknowledge the financial support of National Commission for Scientific and Technological Research (CONICYT) of the Government of Chile through FONDECYT Project 11100495. Support from U-Redes Project, Nanotechnology for Biomedical Applications Network (NanoBioMat), University of Chile is also gratefully acknowledged

References

[1] B.E. Pjetursson, U. Bragger, N.P. Lang, M. Zwahlen, Comparison of survival and complication rates of tooth-supported fixed dental prostheses (FDPs) and implant-supported FDPs and single crowns (SCs), Clin. Oral Implants Res. 3 (2007) 97–113.
[2] B.E. Pjetursson, D. Thoma, R. Jung, M. Zwahlen, A. Zembic, A systematic review of the survival and complication rates of implant-supported fixed dental prostheses (FDPs) after a mean observation period of at least 5 years, Clin. Oral Implants Res. 6 (2012) 22–38.
[3] B.E. Pjetursson, A.G. Asgeirsson, M. Zwahlen, I. Sailer, Improvements in implant dentistry over the last decade: comparison of survival and complication rates in older and newer publications, Int. J. Oral Maxillofac. Implants 29 (2014) 308–324.
[4] C.M. Abraham, A brief historical perspective on dental implants, their surface coatings and treatments, Open Dent. J. 8 (2014) 50–55.
[5] J. Chen, C. Rungsiyakull, W. Li, Y. Chen, M. Swain, Q. Li, Multiscale design of surface morphological gradient for osseointegration, J. Mech. Behav. Biomed. Mater. 20 (2013) 387–397.
[6] D.M. Dohan Ehrenfest, P.G. Coelho, B.S. Kang, Y.T. Sul, T. Albrektsson, Classification of osseointegrated implant surfaces: materials, chemistry and topography, Trends Biotechnol. 28 (2010) 198–206.
[7] P.G. Coelho, J.M. Granjeiro, G.E. Romanos, M. Suzuki, N.R. Silva, G. Cardaropoli, V.P. Thompson, J.E. Lemons, Basic research methods and current trends of dental implant surfaces, J. Biomed. Mater. Res. B: Appl. Biomater. 88 (2009) 579–596.
[8] Z. Schwartz, P. Raz, G. Zhao, Y. Barak, M. Tauber, H. Yao, B.D. Boyan, Effect of micrometer-scale roughness of the surface of Ti6Al4V pedicle screws in vitro and in vivo, J. Bone Joint Surg. Am. 90 (2008) 2485–2498.
[9] A.P. Tomsia, M.E. Launey, J.S. Lee, M.H. Mankani, U.G.K. Wegst, E. Saiz, Nanotechnology approaches to improve dental implants, Int. J. Oral Maxillofac. Implants 26 (2011) 25–44.
[10] S. Lavenus, G. Louarn, P. Layrolle, Nanotechnology and dental implants, Int. J. Biomater. 2010 (2010) 915327.
[11] M. Domanski, R. Luttge, E. Lamers, X.F. Walboomers, L. Winnubst, J.A. Jansen, J.G.E. Gardeniers, Submicron-patterning of bulk titanium by nanoimprint lithography and reactive ion etching, Nanotechnology 23 (2012) 065306.
[12] S.H. Lee, H.W. Kim, E.J. Lee, L.H. Li, H.E. Kim, Hydroxyapatite-TiO_2 hybrid coating on Ti implants, J. Biomater. Appl. 20 (2006) 195–208.

[13] L. Meirelles, F. Currie, M. Jacobsson, T. Albrektsson, A. Wennerberg, The effect of chemical and nanotopographical modifications on the early stages of osseointegration, Int. J. Oral Maxillofac. Implants 23 (2008) 641–647.
[14] K. Ariga, J.P. Hill, M.V. Lee, A. Vinu, R. Charvet, S. Acharya, Challenges and breakthroughs in recent research on self-assembly, Sci. Technol. Adv. Mater. 9 (2008) 014109.
[15] C.J. Brinker, Y.F. Lu, A. Sellinger, H.Y. Fan, Evaporation-induced self-assembly: nanostructures made easy, Adv. Mater. 11 (1999) 579–585.
[16] Y.F. Lu, R. Ganguli, C.A. Drewien, M.T. Anderson, C.J. Brinker, W.L. Gong, Y.X. Guo, H. Soyez, B. Dunn, M.H. Huang, J.I. Zink, Continuous formation of supported cubic and hexagonal mesoporous films by sol–gel dip-coating, Nature 389 (1997) 364–368.
[17] D. Inzunza, C. Covarrubias, A. Von Marttens, Y. Leighton, J.C. Carvajal, F. Valenzuela, M. Díaz-Dosque, N. Méndez, C. Martínez, A.M. Pino, J.P. Rodríguez, M. Cáceres, P. Smith, Synthesis of nanostructured porous silica coatings on titanium and their cell adhesive and osteogenic differentiation properties, J. Biomed. Mater. Res. A 102 (2014) 37–48.
[18] D.L. Wheeler, M.J. Montfort, S.W. McLoughlin, Differential healing response of bone adjacent to porous implants coated with hydroxyapatite and 45S5 bioactive glass, J. Biomed. Mater. Res. 55 (2001) 603–612.
[19] M. Yamada, T. Ueno, N. Tsukimura, T. Ikeda, K. Nakagawa, N. Hori, T. Suzuki, T. Ogawa, Bone integration capability of nanopolymorphic crystalline hydroxyapatite coated on titanium implants, Int. J. Nanomed. 7 (2012) 859–873.
[20] F. Valenzuela, C. Covarrubias, C. Martinez, P. Smith, M. Diaz-Dosque, M. Yazdani-Pedram, Preparation and bioactive properties of novel bone-repair bionanocomposites based on hydroxyapatite and bioactive glass nanoparticles, J. Biomed. Mater. Res. B: Appl. Biomater. 100 (2012) 1672–1682.
[21] T. Kokubo, H. Kushitani, S. Sakka, T. Kitsugi, T. Yamamuro, Solution able to reproduce in vivo surface-structure change in bioactive glass–ceramic A-W, J. Biomed. Mater. Res. 24 (1990) 723–734.
[22] M. Diefenbeck, T. Muckley, C. Schrader, J. Schmidt, S. Zankovych, J. Bossert, D.J. Klaus, M. Faucond, U. Finger, The effect of plasma chemical oxidation of titanium alloy on bone-implant contact in rats, Biomaterials 32 (2011) 8041–8047.
[23] K. Vandamme, X. Holy, M. Bensidhoum, D. Logeart-Avramoglou, I.E. Naert, J.A. Duyck, H. Petite, In vivo molecular evidence of delayed titanium implant osseointegration in compromised bone, Biomaterials 32 (2011) 3547–3554.
[24] S.M. Jeong, B.H. Choi, J. Li, H.S. Kim, C.Y. Ko, J.H. Jung, H.J. Lee, S.H. Lee, W. Engelke, Flapless implant surgery: an experimental study, Oral Surg. Oral Med. Oral Pathol. Oral Radiol. Endodontol. 104 (2007) 24–28.
[25] A.M. Bayounis, H.A. Alzoman, J.A. Jansen, N. Babay, Healing of peri-implant tissues after flapless and flapped implant installation, J. Clin. Periodontol. 38 (2011) 754–761.
[26] J.L. Peris, J. Prat, M. Comin, R. Dejoz, I. Roger, P. Vera, Técnica histológica para la inclusión en metil-metacrilato de muestras óseas no descalcificadas, Rev. Esp. Cir. Osteoart. 28 (1993) 231–238.
[27] Y. Lu, R. Gangull, C.A. Drewlen, M.T. Anderson, C.J. Brinker, W. Gong, Y. Guo, H. Soyez, B. Dunn, M.H. Huang, J.I. Zink, Continuous formation of supported cubic and hexagonal mesoporous films by sol–gel dip-coating, Nature 389 (1997) 36468.
[28] L. Le Guehennec, A. Soueidan, P. Layrolle, Y. Amouriq, Surface treatments of titanium dental implants for rapid osseointegration, Dent. Mater. 23 (2007) 844–854.
[29] H.M. Kim, F. Miyaji, T. Kokubo, T. Nakamura, Effect of heat treatment on apatite-forming ability of Ti metal induced by alkali treatment, J. Mater. Sci. Mater. Med. 8 (1997) 341–347.
[30] T. Kokubo, F. Miyaji, H.M. Kim, T. Nakamura, Spontaneous formation of bonelike apatite layer on chemically treated titanium metals, J. Am. Ceram. Soc. 79 (1996) 1127–1129.
[31] G.M. Luz, J.F. Mano, Preparation and characterization of bioactive glass nanoparticles prepared by sol–gel for biomedical applications, Nanotechnology 22 (2011) 494014.
[32] Z. Hong, R.L. Reis, J.F. Mano, Preparation and in vitro characterization of novel bioactive glass ceramic nanoparticles, J. Biomed. Mater. Res. A 88 (2009) 304–313.
[33] S.K. Misra, D. Mohn, T.J. Brunner, W.J. Stark, S.E. Philip, I. Roy, V. Salih, J.C. Knowles, A.R. Boccaccini, Comparison of nanoscale and microscale bioactive glass on the properties of P(3HB)/bioglass composites, Biomaterials 29 (2008) 1750–1761.
[34] M.J. Dalby, Topographically induced direct cell mechanotransduction, Med. Eng. Phys. 27 (2005) 730–742.
[35] S. Oh, K.S. Brammer, Y.S.J. Li, D. Teng, A.J. Engler, S. Chien, S. Jin, Stem cell fate dictated solely by altered nanotube dimension, Proc. Natl. Acad. Sci. U.S.A. 106 (2009) 2130–2135.
[36] M.J. Dalby, D. McCloy, M. Robertson, C.D. Wilkinson, R.O. Oreffo, Osteoprogenitor response to defined topographies with nanoscale depths, Biomaterials 27 (2006) 1306–1315.
[37] M.J. Dalby, D. McCloy, M. Robertson, H. Agheli, D. Sutherland, S. Affrossman, R.O.C. Oreffo, Osteoprogenitor response to semi-ordered and random nanotopographies, Biomaterials 27 (2006) 2980–2987.
[38] M.J. Dalby, N. Gadegaard, R. Tare, A. Andar, M.O. Riehle, P. Herzyk, The control of human mesenchymal cell differentiation using nanoscale symmetry and disorder, Nat. Mater. 6 (2007) 997–1003.
[39] I.D. Xynos, M.V. Hukkanen, J.J. Batten, L.D. Buttery, L.L. Hench, J.M. Polak, Bioglass 45S5 stimulates osteoblast turnover and enhances bone formation in vitro: implications and applications for bone tissue engineering, Calcif. Tissue Int. 67 (2000) 321–329.
[40] C. Loty, J.M. Sautier, M.T. Tan, M. Oboeuf, E. Jallot, H. Boulekbache, D. Greenspan, N. Forest, Bioactive glass stimulates in vitro osteoblast differentiation and creates a favorable template for bone tissue formation, J. Bone Miner. Res. 16 (2001) 231–239.
[41] O. Tsigkou, J.R. Jones, J.M. Polak, M.M. Stevens, Differentiation of fetal osteoblasts and formation of mineralized bone nodules by 45S5 Bioglass conditioned medium in the absence of osteogenic supplements, Biomaterials 30 (2009) 3542–3550.
[42] C. Covarrubias, F. Arroyo, C. Balanda, I. Celhay, J.P. Rodríguez, M. Díaz, M. Neira, P. Caviedes, In vitro activity and cell differentiation properties of nanobioceramics with different nanostructure, in: 26th European Conference on Biomaterials, Liverpool, UK, 31st August–3rd September 2014, 2014.
[43] Y. Liang, H. Li, J. Xu, X. Li, M. Qi, M. Hu, Morphology, composition, and bioactivity of strontium-doped brushite coatings deposited on titanium implants via electrochemical deposition, Int. J. Mol. Sci. 15 (2014) 9952–9962.
[44] A. Abron, M. Hopfensperger, J. Thompson, L.F. Cooper, Evaluation of a predictive model for implant surface topography effects on early osseointegration in the rat tibia model, J. Prosthet. Dent. 85 (2001) 40–46.
[45] R. Branemark, L.O. Ohrnell, P. Nilsson, P. Thomsen, Biomechanical characterization of osseointegration during healing: an experimental in vivo study in the rat, Biomaterials 18 (1997) 969–978.
[46] C.M. Clokie, H. Warshawsky, Morphologic and radioautographic studies of bone formation in relation to titanium implants using the rat tibia as a model, Int. J. Oral Maxillofac. Implants 10 (1995) 155–165.
[47] T. Masuda, G.E. Salvi, S. Offenbacher, D.A. Felton, L.F. Cooper, Cell and matrix reactions at titanium implants in surgically prepared rat tibiae, Int. J. Oral Maxillofac. Implants 12 (1997) 472–485.
[48] J. Ballarre, R. Seltzer, E. Mendoza, J.C. Orellano, Y.W. Mai, C. Garcia, S.M. Cere, Morphologic and nanomechanical characterization of bone tissue growth around bioactive sol–gel coatings containing wollastonite particles applied on stainless steel implants, Mater. Sci. Eng. C: Mater. Biol. Appl. 31 (2011) 545–552.